Journal of Computational and Applied Mathematics 235 (2011) 2343–2356

Contents lists available at ScienceDirect

Journal of Computational and Applied Mathematics

journal homepage: www.elsevier.com/locate/cam

Uzawa block relaxation method for the unilateral contact problem

Jonas Koko *

Clermont Université, Université Blaise Pascal, LIMOS, BP 10448, F-63000 Clermont-Ferrand, France
CNRS, UMR 6158, LIMOS, F-63173 Aubière, France

ARTICLE INFO

Article history:
Received 28 July 2007
Received in revised form 7 June 2010

Keywords:
Augmented Lagrangian
Linear elasticity
Contact
Friction

ABSTRACT

We present a Uzawa block relaxation method for the numerical resolution of contact problems with or without friction, between elastic solids in small deformations. We introduce auxiliary unknowns to separate the linear elasticity subproblem from the unilateral contact and friction conditions. Applying a Uzawa block relaxation method to the corresponding augmented Lagrangian functional yields a two-step iterative method with a linear elasticity problem as a main subproblem while auxiliary unknowns are computed explicitly. Numerical experiments show that the method are robust and scalable with a significant saving of computational time.

1. Introduction

The contact problem is a very common problem in engineering (rails, gear, forming, etc.). The presence of unilateral and friction constraints poses a serious challenge compared with the classical linear elasticity problem. Various numerical methods for solving unilateral contact problems with or without friction have been developed during the past decades. For frictionless unilateral contact problems, we refer, e.g., to [1–3] and the references therein. For the unilateral contact problem with the Coulomb friction, two main approaches can be considered:

- the direct approach, i.e. the system of discretized equations is solved; see e.g. [4–11].
- The Coulomb friction as the limit of a sequence of the Tresca friction problems; see e.g. [12–14,7,1,15].

Direct approaches are based on finite-dimensional problems and their implementation can be complicated. The second approach is more commonly used and requires fast methods for solving the Tresca friction problems; see e.g. [13–15,2].

The method proposed in this paper is related to the augmented Lagrangian operator-splitting methods; see e.g. [16,17]. The main idea is to separate the linear part of the problem (i.e. linear elasticity) from the nonlinear part (i.e. unilateral contact and friction conditions) by introducing auxiliary variables. Applying a Uzawa block relaxation type method to the corresponding augmented Lagrangian leads to a simple two-step iterative method. In the first step a linear elasticity problem is solved. In the second step, the auxiliary variables are computed explicitly using the duality theory. The main advantage of our method is that the matrix of the linear elasticity problem solved in the first step is constant during the iterative process, saving computational time due to matrix factorizations.

The paper is organized as follows. In Section 2 the model problem is presented followed by its augmented Lagrangian formulation in Section 3. The Uzawa block relaxation algorithms for frictionless and friction cases are presented in Sections 4 and 5, respectively. The convergence theorem of the algorithm is presented in Section 6. Numerical experiments on two model examples are presented in Section 7.

* Corresponding address: CNRS, UMR 6158, LIMOS, F-63173 Aubière, France. Fax: +33 4 73 40 50 01.
E-mail address: koko@sp.isima.fr.

0377-0427/$ – see front matter © 2010 Elsevier B.V. All rights reserved.
doi:10.1016/j.cam.2010.10.032

2. The model problem

We consider an elastic body occupying in its initial (undeformed) configuration a bounded domain Ω of $\mathbb{R}^2$ with a boundary $\Gamma = \Gamma_D \cup \Gamma_c$. We assume that the elastic body is fixed along Γ_D with meas$(\Gamma_D) > 0$. Γ_c denotes a portion of Γ which is a candidate contact surface between Ω and a rigid foundation. The normalized gap between Γ_c and the rigid foundation is denoted by g. In this paper, we consider the small strain hypothesis so that the strain tensor is $\epsilon(u) = (\nabla u + \nabla u^t)/2$, where $u = (u_1(x), u_2(x))$ is the displacement field. Hooke's law is assumed, i.e. the stress tensor is linked to the displacement through the linear relation

$$\sigma(u) = C\epsilon(u)$$

where $C = (C_{ijkl})$ is the (fourth order) elastic moduli tensor, assumed to be symmetric positive definite. Let n be the outward unit normal to Ω on Γ. It is usual to decompose the displacement field and the stress tensor in normal and tangential components:

$$u_n = u \cdot n, \qquad u_t = u - u_n n, \tag{2.1}$$

$$\sigma_n(u) = (\sigma(u)n) \cdot n, \qquad \sigma_t(u) = \sigma(u) - \sigma_n n. \tag{2.2}$$

The unilateral contact problem with Coulomb friction consists, for a given volume force f, of finding the displacement field u satisfying

(i) the equilibrium equations

$$-\mathrm{div}\,\sigma(u) = f \quad \text{in } \Omega, \tag{2.3}$$

$$u = 0 \quad \text{on } \Gamma_D, \tag{2.4}$$

(ii) the contact (i.e. non-penetration) conditions

$$u_n - g \le 0, \qquad \sigma_n(u) \le 0, \qquad (u_n - g)\sigma_n(u) = 0, \quad \text{on } \Gamma_c, \tag{2.5}$$

(iii) the Coulomb friction conditions

$$|\sigma_t(u)| \le \nu_f |\sigma_n(u)|, \qquad |\sigma_t(u)| < \nu_f |\sigma_n(u)| \Longrightarrow u_t = 0 \quad \text{on } \Gamma_c, \tag{2.6}$$

$$|\sigma_t(u)| = \nu_f |\sigma_n(u)| \Longrightarrow \exists \lambda \ge 0, \qquad u_t = -\lambda \sigma_t(u) \quad \text{on } \Gamma_c. \tag{2.7}$$

In (2.6)–(2.7), ν_f stands for the (positive) friction coefficient.

If the normal stress $\sigma_n(u)$ on Γ_c is known, the Coulomb friction conditions (2.6)–(2.7) can be replaced by the Tresca friction conditions

$$s = \nu_f |\sigma_n(u)|, \qquad |\sigma_t(u)| < s \Longrightarrow u_t = 0 \quad \text{on } \Gamma_c, \tag{2.8}$$

$$|\sigma_t(u)| = s \Longrightarrow \exists \lambda \ge 0, \qquad u_t = -\lambda \sigma_t(u) \quad \text{on } \Gamma_c. \tag{2.9}$$

In this paper, we approximate the Coulomb friction (2.6)–(2.7) by solving a sequence of Tresca friction problems. Uzawa block relaxation algorithms are therefore designed for the unilateral frictionless contact problems (2.3)–(2.5) and the unilateral contact problem with Tresca friction (2.3)–(2.5), (2.8)–(2.9).

3. Augmented Lagrangian formulation

The contact problem with Tresca friction can be stated as an optimization problem allowing the use of arguments from convex analysis and duality theory to show the existence of a unique solution and to design numerical algorithms. Let us introduce space of functions

$$V = \left\{ v \in H^1(\Omega)^2, \ v = 0 \text{ on } \Gamma_D \right\}$$

and the set of admissible displacements

$$K = \{ v \in V, \ v_n - g \le 0 \text{ on } \Gamma_c \}.$$

Let $a(\cdot,\cdot)$ be the symmetric, continuous and coercive bilinear form which corresponds to the virtual work in the elastic body

$$a(u, v) = \int_\Omega \sigma_{ij}(u)\epsilon_{ij}(v)\mathrm{d}x.$$

We denote by $f(\cdot)$ the linear form of external forces

$$f(v) = \int_\Omega f \cdot v \mathrm{d}x.$$

In addition, we define the friction functional $j : V \longrightarrow \mathbb{R}$ by

$$j(v) = \int_{\Gamma_c} s|v_t|\mathrm{d}\Gamma, \tag{3.1}$$

where $|\cdot|$ is the Euclidean norm.

Using the above notations, the unilateral contact problem with Tresca friction can be formulated in the variational form.

Find $u \in K$ such that

$$a(u, v-u) + j(v) - j(u) \geq f(v-u), \quad \forall v \in K. \tag{3.2}$$

To formulate (3.2) as a constrained minimization problem, let us introduce the potential energy functional due to non-frictional effects

$$J(v) = \frac{1}{2}a(v, v) - f(v).$$

The quadratic functional J is strictly convex, coercive and Gâteau-differentiable on V. Moreover, the friction functional j is convex and lower semi-continuous on V. We can replace the variational inequality (3.2) by the minimization problem.

Find $u \in K$ such that

$$J(u) + j(u) \leq J(v) + j(v), \quad \forall v \in K. \tag{3.3}$$

Since the functional $J+j$ is strictly convex and coercive ($\mathrm{mes}(\Gamma_D) > 0$), there exists a unique solution to (3.3); see e.g. [1, 10.3]. Note that j being a non-differentiable functional, standard optimization methods cannot be used for solving (3.3).

We can define an augmented Lagrangian to (3.3) but this leads us to Uzawa type algorithms with matrix factorizations in every iteration. To achieve a solution of (3.3) by a Uzawa block relaxation type method, we need additional steps. Following Glowinski and Le Tallec [17], we introduce the set

$$C = \left\{\varphi \in L^2(\Gamma_c),\ \varphi - g \leq 0 \text{ on } \Gamma_c\right\}$$

and its characteristic functional $I_C : L^2(\Gamma_c) \to \mathbb{R} \cup \{+\infty\}$ defined by

$$I_C(\varphi) = \begin{cases} 0 & \text{if } \varphi \in C, \\ +\infty & \text{if } \varphi \notin C. \end{cases}$$

Let us introduce auxiliary variables ϕ_c (contact) and ϕ_f (friction), defined on Γ_c. To simplify, we set $\boldsymbol{\phi} = (\phi_c, \phi_f)$. It is clear that (3.3) is equivalent to the following constrained minimization problem.

Find $(u, \boldsymbol{\phi}) \in V \times (L^2(\Gamma_c))^2$ such that

$$J(u) + j(\phi_f) + I_C(\phi_c) \leq J(v) + j(\varphi_f) + I_C(\varphi_c) \quad \forall (v, \boldsymbol{\varphi}) \in V \times (L^2(\Gamma_c))^2, \tag{3.4}$$

$$u_n - \phi_c = 0 \quad \text{on } \Gamma_c, \tag{3.5}$$

$$u_t - \phi_f = 0 \quad \text{on } \Gamma_c, \tag{3.6}$$

where we have set $\boldsymbol{\varphi} = (\varphi_c, \varphi_f)$. In (3.4), to simplify the presentation, we have implicitly assumed that $I_C(v) = I_C(v_n)$ and $j(v) = j(v_t)$ to avoid using (linear and continuous) operators from V to $L^2(\Gamma_c)$. A more rigorous formulation will be given in Section 6. To introduce an augmented Lagrangian functional, multipliers must belong to $L^2(\Gamma_c)$. We then assume that $f \in L^2(\Omega)$, $s \in L^2(\Gamma_c)$ and Γ_c is sufficiently regular with the additional property that the contact zone is strictly contained in Γ_c; see [18]. We can associate to (3.4)–(3.5) the augmented Lagrangian functional $\mathscr{L}_r$ defined over $V \times (L^2(\Gamma_c))^2 \times (L^2(\Gamma_c))^2$ by

$$\mathscr{L}_r(v, \boldsymbol{\varphi}; \boldsymbol{\mu}) = J(v) + j(\varphi_f) + I_C(\varphi_c) + (\mu_c, v_n - \varphi_c)_{\Gamma_c} + (\mu_f, v_t - \varphi_f)_{\Gamma_c} + \frac{r}{2}\|v_n - \varphi_c\|^2_{0,\Gamma_c} + \frac{r}{2}\|v_t - \varphi_f\|^2_{0,\Gamma_c} \tag{3.7}$$

where $r > 0$ is the (constant) penalty or augmentation parameter and $\boldsymbol{\mu} = (\mu_c, \mu_f)$. Since the functional $J + j$ is strictly convex and the constraints (3.5)–(3.6) are linear, a saddle point of $\mathscr{L}_r$ exists and is the solution of the saddle-point problem.

Find $((u, \boldsymbol{\phi}), \boldsymbol{\lambda}) \in V \times (L^2(\Gamma_c))^2 \times (L^2(\Gamma_c))^2$ such that

$$\mathscr{L}_r(u, \boldsymbol{\phi}; \boldsymbol{\mu}) \leq \mathscr{L}_r(v, \boldsymbol{\varphi}; \boldsymbol{\mu}) \leq \mathscr{L}_r(v, \boldsymbol{\varphi}; \boldsymbol{\lambda}), \quad \forall ((v, \boldsymbol{\varphi}), \boldsymbol{\mu}) \in V \times (L^2(\Gamma_c))^2 \times (L^2(\Gamma_c))^2,$$

where we have set $\boldsymbol{\lambda} = (\lambda_c, \lambda_f)$. Equivalently, $((u, \boldsymbol{\phi}), \boldsymbol{\lambda})$ is the solution of the min–max problem

$$\max_{\boldsymbol{\mu}} \min_{(v, \boldsymbol{\varphi})} \mathscr{L}_r(v, \boldsymbol{\varphi}; \boldsymbol{\mu}) = \min_{(v, \boldsymbol{\varphi})} \max_{\boldsymbol{\mu}} \mathscr{L}_r(v, \boldsymbol{\varphi}; \boldsymbol{\mu}).$$

The Lagrange multipliers λ_c and λ_f have the following mechanical interpretation:

- λ_c is the negative normal boundary stress, i.e. $\lambda_c = -\sigma_n(u)$;
- λ_f is the negative tangential boundary stress, i.e. $\lambda_f = -\sigma_t(u)$.

It suffices to eliminate auxiliary unknowns, using (3.5)–(3.6), so that λ_c and λ_f become classical Lagrange multipliers associated with the non-penetration and friction conditions, respectively. An advantage of Uzawa type methods is that the normal and the tangential boundary stress are available, in the form of Lagrange multipliers, at the end of the algorithm without additional calculations.

4. Uzawa block relaxation method: frictionless case

In this section we consider the augmented Lagrangian functional

$$\mathscr{L}_r(v, \varphi_c; \mu_c) = J(v) + I_C(\varphi_c) + (\mu_c, v_n - \varphi_c)_{\Gamma_c} + \frac{r}{2}\|v_n - \varphi_c\|^2_{0,\Gamma_c} \tag{4.1}$$

i.e. the frictionless version of (3.7). A saddle point of $\mathscr{L}_r$ can be determined by a standard Uzawa method for augmented Lagrangian; see e.g. [19]. The main difficulty of the standard Uzawa method is the coupling of unknowns u and ϕ_c, i.e. the "linear part" and the "nonlinear part" of the problem. A quite natural procedure consists of using the following Uzawa block relaxation method [16,17].

Initialization. ϕ_c^{-1} and λ_c^0 are given.
Iteration $k \geq 0$. Compute successively u^k, ϕ_c^k and λ_c^{k+1} as follows

- Find $u^k \in V$ such that
$$\mathscr{L}_r(u^k, \phi_c^{k-1}; \lambda_c^k) \leq \mathscr{L}_r(v, \phi_c^{k-1}; \lambda_c^k), \quad \forall v \in V. \tag{4.2}$$
- Find $\phi_c^k \in L^2(\Gamma_c)$ such that
$$\mathscr{L}_r(u^k, \phi_c^k; \lambda_c^k) \leq \mathscr{L}_r(u^k, \varphi; \lambda_c^k), \quad \forall \varphi \in L^2(\Gamma_c). \tag{4.3}$$
- Update the Lagrange multiplier
$$\lambda_c^{k+1} = \lambda_c^k + r(u_n^k - \phi_c^k). \tag{4.4}$$

We detail in the next subsections subproblems (4.2) and (4.3).

4.1. Solution of subproblem (4.2)

The functional $v \mapsto \mathscr{L}_r(v, \phi_c^{k-1}; \lambda_c^k)$ is Gâteau-differentiable on V, then the solution of (4.2) can be characterized by the Euler–Lagrange equation

$$\frac{\partial}{\partial v}\mathscr{L}_r(u^k, \phi_c^{k-1}; \lambda_c^k) \cdot v = 0, \quad \forall v \in V.$$

A straightforward calculation yields

$$a(u^k, v) + r(u_n^k, v_n)_{\Gamma_c} = f(v) + (r\phi_c^{k-1} - \lambda_c^k, v_n)_{\Gamma_c}, \quad \forall v \in V. \tag{4.5}$$

Subproblem (4.5) is the variational formulation of the problem

$$-\mathrm{div}(\sigma(u^k)) = f \quad \text{in } \Omega, \tag{4.6}$$
$$\sigma_n(u^k) + ru_n^k = r\phi_c^{k-1} - \lambda_c^k \quad \text{on } \Gamma_c, \tag{4.7}$$
$$u^k = 0 \quad \text{on } \Gamma_D. \tag{4.8}$$

Note that the above problem always has a unique solution even without the Dirichlet condition (4.8). This property is useful for solving problems allowing rigid body motions.

4.2. Solution of subproblem (4.3)

Over C the functional $\varphi \mapsto \mathscr{L}_r(u^k, \varphi; \lambda_c^k)$ can be simplified

$$\mathscr{L}_r(u^k, \varphi; \lambda_c^k) = \frac{r}{2}\|\varphi\|^2_{0,\Gamma_c} - (\lambda_c^k + ru_n^k, \varphi)_{\Gamma_c} + J(u^k) + \frac{r}{2}\|u_n^k\|^2_{0,\Gamma_c} + (\lambda_c^k, u_n^k)_{\Gamma_c}.$$

If we denote by α the constant part of $\mathscr{L}_r(u^k, \varphi; \lambda_c^k)$ and we set

$$F(\varphi) = \frac{r}{2}\|\varphi\|^2_{0,\Gamma_c} - (\lambda_c^k + ru_n^k, \varphi)_{\Gamma_c} + \alpha,$$

the minimization problem (4.3) becomes
Find $\phi_c^k \in L^2(\Gamma_c)$ such that

$$F(\phi_c^k) \leq F(\varphi), \quad \forall \varphi \in L^2(\Gamma_c), \tag{4.9}$$
$$\phi_c^k - g \leq 0 \quad \text{on } \Gamma_c. \tag{4.10}$$

Since (4.9)–(4.10) is a constrained minimization problem, we can apply saddle-point theory to compute its solution explicitly. The solution ϕ_c^k of (4.9)–(4.10) satisfies the saddle-point equations

$$r(\phi_c^k, \varphi)_{\Gamma_c} - (ru_n^k + \lambda_c^k, \varphi)_{\Gamma_c} + (\gamma^k, \varphi)_{\Gamma_c} = 0, \quad \forall \varphi \in L^2(\Gamma_c), \tag{4.11}$$

$$(\gamma^k, \phi_c^k - g)_{\Gamma_c} = 0, \tag{4.12}$$

where $\gamma^k \geq 0$ is the Lagrange multiplier for (4.10) (see e.g. [20]). Since $\phi_c^k - g \leq 0$ and $\gamma^k \geq 0$, Eq. (4.12) is equivalent to the statement that γ^k may be nonzero at a point of Γ_c if the corresponding constraint is active, i.e. $\phi_c^k - g = 0$.

From (4.11) we deduce that

$$\phi_c^k = \frac{1}{r}\left(\lambda_c^k + ru_n^k - \gamma^k\right). \tag{4.13}$$

Substituting this result into (4.12), we obtain

$$\left(\gamma^k, \frac{1}{r}\left(\lambda_c^k + ru_n^k - \gamma^k\right) - g\right)_{\Gamma_c} = 0.$$

If $\gamma^k > 0$, we must have

$$\lambda_c^k + ru_n^k - \gamma^k - rg = 0.$$

We deduce that the Lagrange multiplier is

$$\gamma^k = \max(0, \lambda_c^k + r(u_n^k - g)) = \left(\lambda_c^k + r(u_n^k - g)\right)^+. \tag{4.14}$$

Substituting (4.14) into (4.13) we get the solution of the contact minimization subproblem

$$\phi_c^k = u_n^k + \frac{1}{r}\left[\lambda_c^k - \left(\lambda_c^k + r(u_n^k - g)\right)^+\right]. \tag{4.15}$$

Remark 4.1. Note that if $\gamma^k(x) > 0$, then $\phi_c^k(x) = g(x)$, i.e. the contact constraint is active. If $\gamma^k(x) = 0$, then from (4.14)–(4.15) we have $\lambda_c^k + ru_n^k \leq rg$ and $\phi_c^k = (\lambda_c^k + ru_n^k)/r$. We then deduce that

$$\phi_c^k - g = \frac{1}{r}(\lambda_c^k + ru_n^k) - g \leq 0$$

i.e. constraint (4.10) is satisfied.

4.3. Algorithm

With the above preparations, we can now present our Uzawa block relaxation (UBR) method for the unilateral frictionless contact problem.

Algorithm UBR-C

Initialization. ϕ_c^{-1} and λ_c^0 are given.
Iteration $k \geq 0$. Compute successively u^k, ϕ_c^k and λ_c^{k+1} as follows

- Find $u^k \in V$ such that
$$a(u^k, v) + r(u_n^k, v_n)_{\Gamma_c} = f(v) + (r\phi_c^{k-1} - \lambda_c^k, v_n)_{\Gamma_c}, \quad \forall v \in V.$$
- Compute the auxiliary contact variable
$$\phi_c^k = u_n^k + \frac{1}{r}\left[\lambda_c^k - \left(\lambda_c^k + r(u_n^k - g)\right)^+\right].$$
- Update the Lagrange multiplier
$$\lambda_c^{k+1} = \lambda_c^k + r(u_n^k - \phi_c^k).$$

We iterate until the relative error on u^k and ϕ_c^k is "sufficiently" small, i.e.

$$\frac{\|u^k - u^{k-1}\|_{0,\Omega}^2 + \|\phi_c^k - \phi_c^{k-1}\|_{0,\Gamma_c}^2}{\|u^k\|_{0,\Omega}^2 + \|\phi_c^k\|_{0,\Gamma_c}^2} < \varepsilon_c^2. \tag{4.16}$$

Note that for the linear elasticity subproblem, the corresponding matrix is constant during the iterative process.

5. Uzawa block relaxation method: Tresca friction case

We now consider the augmented Lagrangian functional (3.7). Using the block relaxation strategy, we obtain the following algorithm.

Initialization. $\boldsymbol{\phi}^{-1} = (\phi_c^{-1}, \phi_f^{-1})$ and $\boldsymbol{\lambda}^0 = (\lambda_c^0, \lambda_f^0)$ are given.
Iteration $k \geq 0$. Compute successively u^k, $\boldsymbol{\phi}^k = (\phi_c^k, \phi_f^k)$ and $\boldsymbol{\lambda}^{k+1} = (\lambda_c^{k+1}, \lambda_f^{k+1})$ as follows

- Find $u^k \in V$ such that
$$\mathscr{L}_r(u^k, \boldsymbol{\phi}^{k-1}; \boldsymbol{\lambda}^k) \leq \mathscr{L}_r(v, \boldsymbol{\phi}^{k-1}; \boldsymbol{\lambda}^k), \quad \forall v \in V. \tag{5.1}$$
- Find $\boldsymbol{\phi}^k \in (L^2(\Gamma_c))^2$ such that
$$\mathscr{L}_r(u^k, \boldsymbol{\phi}^k; \boldsymbol{\lambda}^k) \leq \mathscr{L}_r(u^k, \boldsymbol{\varphi}; \boldsymbol{\lambda}^k), \quad \forall \boldsymbol{\varphi} \in (L^2(\Gamma_c))^2. \tag{5.2}$$
- Update the Lagrange multipliers
$$\lambda_c^{k+1} = \lambda_c^k + r(u_n^k - \phi_c^k),$$
$$\lambda_f^{k+1} = \lambda_f^k + r(u_t^k - \phi_f^k).$$

Since $v \mapsto \mathscr{L}_r(v, \boldsymbol{\phi}^{k-1}; \boldsymbol{\lambda}^k)$ is Gâteau-differentiable, the solution of problem (5.1) can be characterized by the Euler–Lagrange equation

$$a(u^k, v) + r(u_n^k, v_n)_{\Gamma_c} + r(u_t^k, v_t)_{\Gamma_c} = f(v) + (r\phi_c^{k-1} - \lambda_c^k, v_n)_{\Gamma_c} + (r\phi_f^{k-1} - \lambda_f^k, v_t)_{\Gamma_c}, \quad \forall v \in V. \tag{5.3}$$

The subproblem in $\boldsymbol{\phi} = (\phi_c, \phi_f)$ (5.2) is uncoupled. The subproblem in ϕ_c has been solved in Section 4 and the solution is (4.15). The subproblem in ϕ_f is equivalent to the minimization of the following functional

$$F(\varphi) = \frac{r}{2}\|\varphi\|_{0,\Gamma_c}^2 + \int_{\Gamma_c} s|\varphi| \mathrm{d}\Gamma - (\lambda_f^k + ru_t^k, \varphi)_{\Gamma_c} + \alpha, \tag{5.4}$$

where α is a constant which does not count in the minimization. The infimum of the functional (5.4) is attained at (see e.g. [21, ch. 4.3])

$$\phi_f^k = \begin{cases} \dfrac{|\lambda_f^k + ru_t^k| - s}{r|\lambda_f^k + ru_t^k|}\left(\lambda_f^k + ru_t^k\right) & \text{if } |\lambda_f^k + ru_t^k| > s, \\ 0 & \text{if } |\lambda_f^k + ru_t^k| \leq s. \end{cases} \tag{5.5}$$

Gathering the results (5.3), (4.15) and (5.5), we obtain the following Uzawa block relaxation algorithm for a unilateral contact problem with the Tresca friction.

Algorithm UBR-TF

Initialization. $\boldsymbol{\phi}^{-1} = (\phi_c^{-1}, \phi_f^{-1})$ and $\boldsymbol{\lambda}^0 = (\lambda_c^0, \lambda_f^0)$ are given.
Iteration $k \geq 0$. Compute successively u^k, $\boldsymbol{\phi}^k = (\phi_c^k, \phi_f^k)$ and $\boldsymbol{\lambda}^{k+1} = (\lambda_c^{k+1}, \lambda_f^{k+1})$ as follows

- Find $u^k \in V$ such that
$$a(u^k, v) + r(u_n^k, v_n)_{\Gamma_c} + r(u_t^k, v_t)_{\Gamma_c} = f(v) + (r\phi_c^{k-1} - \lambda_c^k, v_n)_{\Gamma_c} + (r\phi_f^{k-1} - \lambda_f^k, v_t)_{\Gamma_c}, \quad \forall v \in V.$$
- Compute the auxiliary contact and friction variables
$$\phi_c^k = u_n^k + \frac{1}{r}\left[\lambda_c^k - (\lambda_c^k + r(u_n^k - g))^+\right],$$
$$\phi_f^k = \begin{cases} \dfrac{|\lambda_f^k + ru_t^k| - s}{r|\lambda_f^k + ru_t^k|}\left(\lambda_f^k + ru_t^k\right) & \text{if } |\lambda_f^k + ru_t^k| > s, \\ 0 & \text{if } |\lambda_f^k + ru_t^k| \leq s. \end{cases}$$
- Update the Lagrange multipliers
$$\lambda_c^{k+1} = \lambda_c^k + r(u_n^k - \phi_c^k),$$
$$\lambda_f^{k+1} = \lambda_f^k + r(u_t^k - \phi_f^k).$$

We iterate until the relative error on u^k, ϕ_c^k and ϕ_f^k is sufficiently "small", i.e.

$$\frac{\|u^k - u^{k-1}\|_{0,\Omega}^2 + \|\boldsymbol{\phi}^k - \boldsymbol{\phi}^{k-1}\|_{0,\Gamma_c}^2}{\|u^k\|_{0,\Omega}^2 + \|\boldsymbol{\phi}^k\|_{0,\Gamma_c}^2} < \varepsilon_f^2. \tag{5.6}$$

As for the frictionless case, the matrix of the linear elasticity subproblem is constant during the iterative process.

With the solution $(u, \boldsymbol{\phi}, \boldsymbol{\lambda})$ obtained using Algorithm UBR-TF we can update the friction functional j in (3.1) by replacing s by the newly computed contact pressure, i.e. $s = \nu_f|\lambda_c|$. This process is repeated until the difference between two consecutive values of s becomes sufficiently "small". Then the corresponding displacement field u can be identified with the solution of the original unilateral contact problem with Coulomb friction (2.3)–(2.7). This idea is commonly used to calculate the solution of the Coulomb friction problem by a sequence of Tresca friction problems; see e.g. [12–14,22,1,15]. The corresponding fixed-point algorithm is as follows.

Algorithm CF-FP

Iteration $m = 0$. Initialization: s^0 given in $L^2(\Gamma_c)$.
Iteration $m \geq 0$. Compute successively $(u^m, \boldsymbol{\phi}^m, \boldsymbol{\lambda}^m)$ and s^{m+1} as follows

- Compute $(u^m, \boldsymbol{\phi}^m; \boldsymbol{\lambda}^m)$ solution of the Tresca friction problem (3.3) with s^m the normal stress.
- Update the friction functional with $s^{m+1} = \nu_f|\lambda_c^m|$.

The fixed-point iteration terminates if the relative error on s^m becomes sufficiently "small", *i.e.*

$$\frac{\|s^m - s^{m-1}\|_{0,\Gamma_c}^2}{\|s^m\|_{0,\Gamma_c}^2} < \varepsilon_{fp}^2. \tag{5.7}$$

Note that, the matrix of the linear elasticity subproblem is constant during the fixed-point iterations. For the first steps of Algorithm CF-FP, we do not need high accuracy in solving the Tresca friction subproblems. Indeed, we only need an approximate value of the normal stress.

6. Convergence results

In this section, we show the convergence of the Uzawa block relaxation algorithm presented in the previous section. Let us set

$$G(v) = J(v) \quad \text{and} \quad F(\boldsymbol{\varphi}) = j(\varphi_f) + I_C(\varphi_c)$$

and introduce the linear and continuous operator B, from V to $L^2(\Gamma_c) \times L_T^2(\Gamma_c)$, defined by

$$Bv = \begin{pmatrix} v_n \\ v_t \end{pmatrix}$$

where

$$L_T^2(\Gamma_c) = \left\{ v \in (L^2(\Gamma_c))^2 \mid v_n = 0 \right\}.$$

The decomposition $v \to (v_n, v_t)$ is an isomorphism from $(L^2(\Gamma_c))^2$ onto $L^2(\Gamma_c) \times L_T^2(\Gamma_c)$, [1, ch. 5]. It is obvious that (3.3) is equivalent to

Find $u \in V$ such that

$$G(u) + F(Bu) \leq G(v) + F(Bv), \quad \forall v \in V.$$

The functional G is convex, proper and lower semi-continuous while F is strictly convex and continuous. Furthermore, G is uniformly convex on the bounded sets of $\boldsymbol{V}$. Algorithm UBR-TF is therefore equivalent to the operator-splitting standard Algorithm ALG 2 described, e.g., in [17, ch. 3] or [16, ch. 3]. We have the following convergence theorem; see e.g. [17, ch. 3,Theorem 4.2].

Theorem 6.1 (*Convergence*). *The sequence* $(u^k, \boldsymbol{\phi}^k, \boldsymbol{\lambda}^k)$ *generated in Algorithm UBR-TF is such that*

$$u^k \to u \quad \text{in } V, \qquad \boldsymbol{\phi}^k \to \boldsymbol{\phi} \quad \text{in } (L^2(\Gamma_c))^2, \qquad \boldsymbol{\lambda}^k \rightharpoonup \boldsymbol{\lambda} \quad \text{in } (L^2(\Gamma_c))^2,$$

$(u, \boldsymbol{\phi}, \boldsymbol{\lambda})$ *being a saddle point of* $\mathscr{L}_r$.

In the generic operator-splitting Algorithm ALG 2, the convergence is proved by assuming the multiplier update of the form

$$\lambda_c^{k+1} = \lambda_c^k + \rho(u_n^k - \phi_c^k), \qquad \lambda_f^{k+1} = \lambda_f^k + \rho(u_t^k - \phi_f^k),$$

and $0 < \rho < r(1 + \sqrt{5})/2$. But numerical experiments indicate that the best choice for the step size is $\rho = r$.

7. Numerical experiments

Algorithms UBR-C, UBR-TF and CF-FP of the previous sections were implemented in MATLAB 7 on a Linux workstation with 2.67 GHz clock frequency and 12 GB RAM. The test problems used are designed to illustrate the behavior of the algorithms more than to model contact actual phenomena.

We compare Algorithm UBR-C with the semi-smooth Newton method; see e.g. [2,23] which can be expressed as the following active set strategy with respect to the inequality $u_n - g \leq 0$:

Algorithm SSN-C

(1) Choose $u^0 \in V$ and set $k \leftarrow 0$.
(2) Determine

$$\mathcal{A}^{k+1} = \left\{ x \in \Gamma_c \hat{\lambda} + r(u_n^k - g) > 0 \right\},$$
$$\mathcal{I}^{k+1} = \Gamma_c \setminus \mathcal{A}^{k+1}$$

(3) if $k \geq 1$ and $\mathcal{A}^{k+1} = \mathcal{A}^k$ stop, else
(4) Solve

$$a(u^{k+1}, v) + (\hat{\lambda} + r(u_n^{k+1} - g), \chi^{k+1} v_n)_{\Gamma_c} = f(v), \quad \forall v \in V. \tag{7.1}$$

Set $\lambda_c^{k+1} = \begin{cases} \hat{\lambda} + r(u_n^{k+1} - g) & \text{on } \mathcal{A}^{k+1} \\ 0 & \text{on } \mathcal{I}^{k+1} \end{cases}$
and $k \leftarrow k + 1$ and go to Step 2.

In Algorithm SSN-C, $\hat{\lambda} \in L^2(\Gamma_c)$, and $\chi^{k+1} = \chi_{\mathcal{A}^{k+1}}$ is the characteristic function of $\mathcal{A}^{k+1} \subset \Gamma_c$. In numerical experiments, we use $\hat{\lambda} = 0$. The convergence of Algorithm SSN-C is locally superlinear [24,2]. But since the active set changes from one iteration to another in (7.1), the matrix of the linear system must be factorized at each iteration.

Implementation: Implementation of all algorithms are done in Matlab using piecewise linear finite element and vectorized codes [25]. Since the matrix of the linear elasticity subproblem is symmetric positive definite, we use the Cholesky factorization (Matlab function `chol`) after column and row permutations (Matlab function `symamd`) to reduce fill-in. The Cholesky factorization is performed in the first iteration for UBR-C, UBR-TF and CF-FP; so that, during the iterative process, the linear elasticity subproblems reduce to forward/backward substitutions. For the semi-smooth Newton Algorithm SSN-C, a column and row permutation is performed in the first iteration since the locations of nonzero entries of the matrix do not change.

Stopping criteria: The tolerances in the stopping criteria (4.16), (5.6) and (5.7) are

$$\varepsilon_c = 10^{-5}, \qquad \varepsilon_f = 10^{-5}, \qquad \varepsilon_{fp} = 10^{-4},$$

respectively. To make sure that the algorithms converge, we also check if the L^2-norm of the residual is less than 10^{-3}. This value is sufficient and choosing a higher accuracy for the residual increases excessively the number of iterations. For the Tresca friction subproblems solved in Algorithm CF-FP we use the following variable tolerance strategy

$$\varepsilon_f^m = \max\{(0.1)^m, 10^{-5}\},$$

where m is the corresponding fixed-point iteration.

Initialization: For the initialization of UBR algorithms, we simply set $\boldsymbol{\phi}^{-1} = 0$ and $\boldsymbol{\lambda}^0 = 0$. In the first example (Section 7.1), the problem allows rigid body motions in the vertical direction. Fortunately, in our Uzawa block relaxation algorithm the mass terms provided by normal and tangential integrals in (4.5) and (5.3) prevent infinite displacements at the initial step. For Algorithm SSN-C, we have set $\lambda_c^0 = 0$ and $u^0 = (0, -0.01)$ in the initialization step to prevent infinite displacements.

7.1. Example 1: a Hertz problem

A classical test in the numerical simulation of unilateral contact problems is the Hertz contact problem; see e.g. [26,1]. Let us consider an infinitely long cylinder resting in a rigid foundation, and subjected to a uniform load along its top of intensity $g = (0, -1600)$ (units of force per unit area). The radius of the cylinder is $R = 8$. The cylinder is made from a homogeneous, isotropic, elastic material with Young's modulus $E = 2000$ and Poisson's ratio $\nu = 0.3$. The Hertz solution yields a contact pressure of

$$p(x) = \frac{2|g|}{\pi b^2}\sqrt{b^2 - x_1^2}, \tag{7.2}$$

where b is the half-width of the contact surface defined by

$$b = 2\sqrt{|g|R(1-\nu^2)/(\pi E)}.$$

For symmetry reasons, only quarter of the cylinder section is consider in the finite element discretization; see Fig. 1. The contact surface is $\Gamma_c = (0, 8) \times \{0\}$ and we prescribed $u_1 = 0$ on $\Gamma_D = \{0\} \times (0, 8)$ for symmetry.

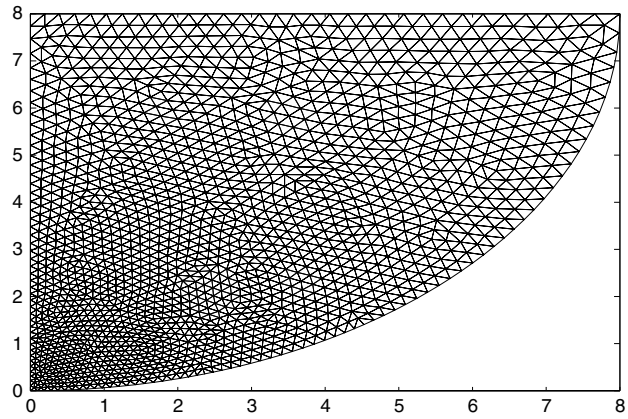

Fig. 1. Sample mesh of a Hertz contact problem.

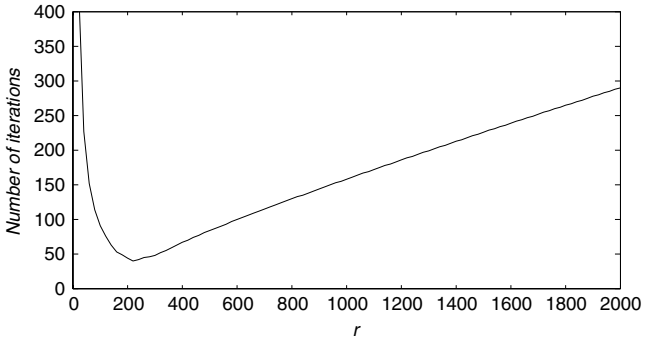

Fig. 2. Number of iterations versus penalty parameter.

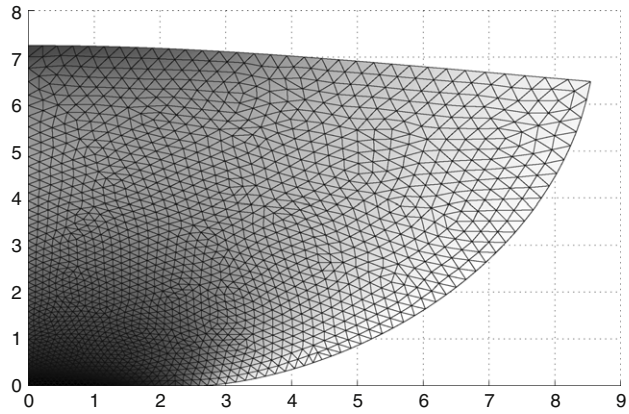

Fig. 3. Deformed configuration and the von Mises stress distribution.

7.1.1. Frictionless case

The Uzawa type algorithms are very sensitive to the choice of the penalty (or augmentation) parameter r. For elasticity problems, we can assume that the penalty parameter is of the form $r = \alpha E$, where $\alpha > 0$ and E is Young's modulus. We then run Algorithm UBR-C with various values of α using a mesh with 1692 nodes and 3236 triangles. Fig. 2 shows the number of iterations versus the penalty parameter r. The "optimal" penalty value is $r \approx 220 = 0.11E$. Choosing larger values for r increases the number of iterations without improving the final result. Fig. 3 shows the deformed configuration. The gray tones visualize the von Mises effective stress distribution in Ω.

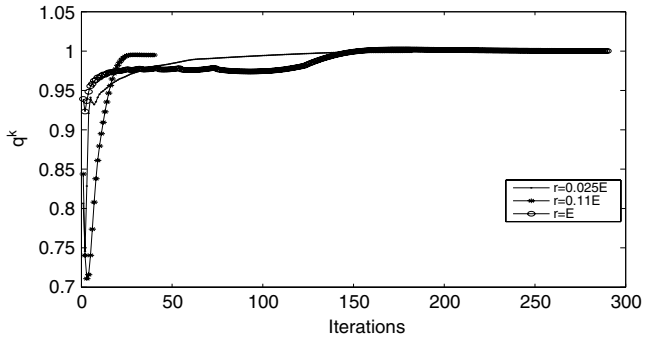

Fig. 4. Relative error q^k of the Lagrange multiplier versus k for Algorithm UBR-C on the frictionless Hertz contact problem.

Table 1
Performances of Algorithms UBR-C ($r = 0.11E$) and SSN-C ($r = 10^3E$) on a Hertz problem without friction.

Mesh nodes Ω/Γ_c	UBR-C		SSN-C	
	Iterations	CPU (s)	Iterations	CPU (s)
442/35	47	0.04	7	0.06
1692/69	40	0.54	8	0.760
6619/137	46	1.34	9	4.72
26 181/271	45	6.83	10	23.270
37 473/329	47	8.90	10	36.190

Table 2
$\|\lambda_c^k - p\|_{L^2(\Gamma_c)}$ for UBR-C and SSN-C.

UBR-C	r	1	$0.11E$	E	$10E$
	$\|\lambda_c - p\|_{0,\Gamma_c}$	24.9455	23.9717	18.5664	17.7830
SSN-C	r	E	10^3E	10^5E	10^8E
	$\|\lambda_c - p\|_{0,\Gamma_c}$	187.0743	35.0988	35.9586	35.9572

We now investigate the rate of convergence of Algorithm UBR-C. In Fig. 4, we plot the relative error of the Lagrange multiplier

$$q^k = \frac{\|\lambda_c^k - p\|_{0,\Gamma_c}}{\|\lambda_c^{k-1} - p\|_{0,\Gamma_c}}$$

versus the iteration number k for various penalty parameters, using the Hertz contact pressure (7.2) as the exact Lagrange multiplier. In Fig. 4, the limit values, for q^k, are 0.9985 (for $r = 0.025E$), 0.9950 (for $r = 0.11E$) and 1.0000 (for $r = E$). We observe a linear rate of convergence of Algorithm UBR-C (as predicted in [16, chap. 9]), for "small" values of r. For "large" values of r (e.g. $r = E$), the convergence of Algorithm UBR-C becomes sublinear.

We now compare the Uzawa block relaxation algorithm for frictionless contact problems (UBR-C) and the semi-smooth Newton algorithm (SSN-C). For Algorithm SSN-C, we made the following observations relative to the Hertz problem under consideration.

- The active set does not change any more for $r \geq 2.5 \times 10^4 = 12.5E$.
- The number of iterations increases moderately with r and the number of mesh nodes.

Ito and Kunisch [27, Section 4] observe the same behavior for several examples with smooth problem data. For these reasons, we do not use specific techniques such as path following [23] for this class of problems. We report in Table 1 the number of iterations and CPU time of both algorithms for different mesh sizes. We first notice that, for Algorithm UBR-C, the number of iterations required for convergence is virtually independent of the mesh size. We also notice that Algorithm SSN-C requires more CPU time than Algorithm UBR-C, because of matrix factorizations in every iteration. The saving of computational cost obtained with Algorithm UBR-C is therefore significant. For the largest problem, Algorithm UBR-C is more than 4 times faster than Algorithm SSN-C.

Fig. 5 shows numerical and analytical contact pressure distributions on Γ_c. We notice that the contact pressure obtained with both algorithms coincide except at the boundary of the contact area. In Table 2 we report L^2-norm of the difference between λ_c^k (obtained with UBR-C or SSN-C) and the Hertz contact pressure (7.2). We can notice that Algorithm UBR-C is more robust and accurate. The robustness of Algorithm UBR-C follows from Theorem 6.1 which is valid for any $r > 0$. For $r = 1$, Algorithm UBR-C requires 8977 iterations while the number of iterations is only 40 for $r = 0.11E$. But in both cases,

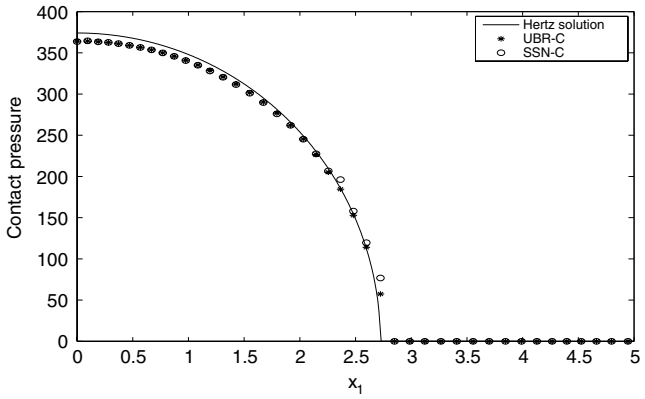

Fig. 5. Contact pressure distributions for a Hertz problem.

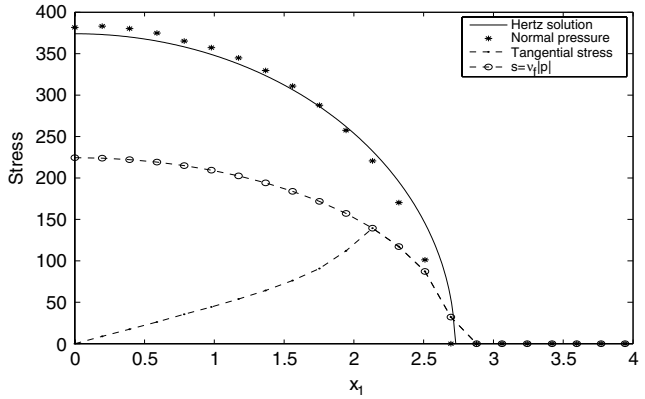

Fig. 6. Stress distributions for a Hertz problem with the Tresca friction.

Table 3
Performances of Algorithm UBR-TF on a Hertz problem with the Tresca friction.

Mesh nodes Ω/Γ_c	Iterations	CPU (in s)
442/35	57	0.04
1692/69	47	0.55
6619/137	51	1.68
26 181/273	50	7.54
37 473/329	48	9.79

the solution obtained is an approximate solution of the original contact problem. This is not the case for Algorithm SSN-C since it converges towards the solution of the *regularized problem*.

7.1.2. Friction case

We now study, the behavior of Algorithm UBR-TF on a Hertz problem with the Tresca friction. The friction coefficient is $\nu_f = 0.6$ and the known normal stress is the Hertz contact pressure (7.2). Using a mesh with 1692 nodes and studying the evolution of the number of iterations versus the penalty parameter, we determine the "optimal" penalty parameter $r \approx 260 = 0.13E$.

In Table 3 we report the performances of Algorithm UBR-TF. We notice that the number of iterations is virtually independent of the mesh size. Fig. 6 shows the stress distributions on Γ_c. One can notice that, compared to the frictionless case, the maximum contact pressure increases while the contact area is reduced. The sticking zone ($|\lambda_f| < \nu_f|p|$) and the sliding zone ($|\lambda_f| = \nu_f|p|$) are clearly identified. Note that the tangential stress has a sort of singular point at the end of the sticking zone as observed e.g. by [1]. It is interesting to notice that, for the largest problem, the computational cost of Algorithm UBR-TF is only (about) 10% higher than the frictionless case.

We now study the behavior of the fixed-point Algorithm CF-FP on the Hertz problem with the Coulomb friction. The penalty parameter is $r = 580 = 0.29E$ in Algorithm UBR-TF used as the Tresca friction solver. We report in Table 4 the

Table 4
Performances of Algorithm CF-FP on a Hertz problem with the Coulomb friction.

Mesh nodes	Fixed-point iterations	Tresca iterations	CPU (in s)
442	9	109	0.08
1692	8	106	0.81
6619	13	122	2.51
26 181	11	115	14.41
37 473	10	114	20.53

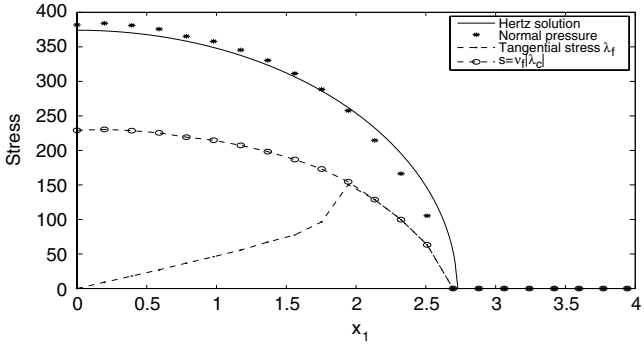

Fig. 7. Stress distributions for a Hertz problem with the Coulomb friction.

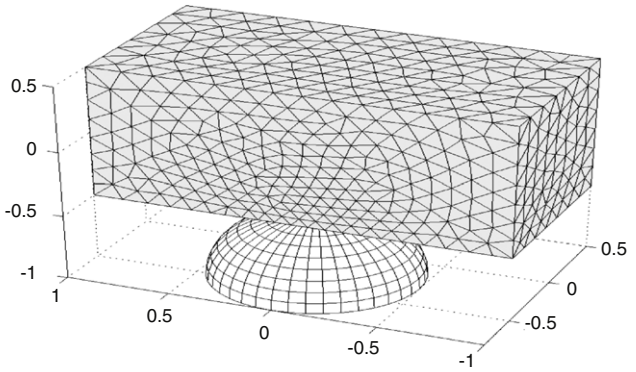

Fig. 8. Geometry and obstacle for the three-dimensional problem.

performances of Algorithm CF-FP in terms of inner/outer iterations and CPU time. One can notice again that the number of iterations (inner or outer) is virtually independent of the mesh size. Fig. 7 shows the stress distribution on Γ_c with the same properties as for the Tresca friction case, Fig. 6.

7.2. Example 2: a three-dimensional problem

In this example, we study the behavior of a three-dimensional rectangular elastic body pressed onto a solid hemisphere, [23]. The elastic body occupies the domain $\Omega = (-0.5, 0.5) \times (-1, 1) \times (-0.5, 0.5)$ with elastic constants $E = 10^6$ and $\nu = 0.45$. The obstacle is a half-ball with radius $r = 0.5$ and center $(-0.3, 0, -1)$. Fig. 8 shows the geometry of the problem. A displacement $u_D = (0, 0, -0.2)$ is prescribed on the upper surface $\Gamma_D = (-0.5, 0.5) \times (-1, 1) \times \{0.5\}$. The contact surface is the lower surface $\Gamma_c = (-0.5, 0.5) \times (-1, 1) \times \{-0.5\}$ with $u_n = u_3$ and $u_t = (u_1, u_2, 0)^T$. Then, in (5.5), $|\cdot|$ stands for the Euclidean norm.

Using the same procedure as in Section 7.1, we obtain as "optimal" penalty parameters $r \approx 4E$ (for the frictionless case), $r \approx 2.75E$ (for the Tresca friction case) and $r = 6.25E$ (for the Coulomb friction case), using a mesh with 739 nodes and 3284 tetrahedrons.

7.2.1. Frictionless case

Algorithm UBR-C stops after 40 iterations using a mesh with 739 nodes and 3284 tetrahedrons; see Fig. 8. Fig. 9 shows the deformed mesh, gray tones visualize the vertical component of the second order Cauchy stress tensor, i.e. $\sigma_{33}(u)$ in the three-dimensional case. Fig. 10 shows the normal stress (σ_n) distribution on the contact surface Γ_c.

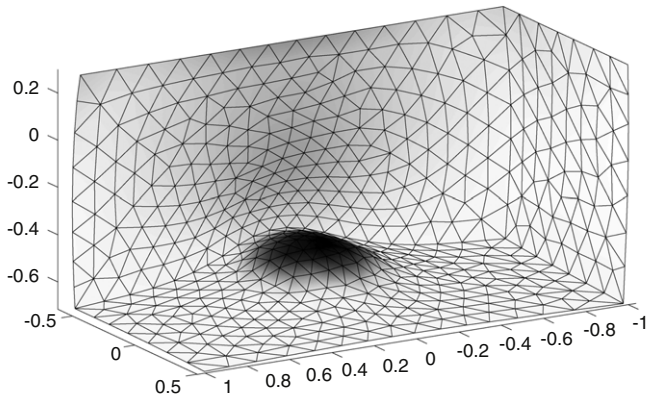

Fig. 9. Deformed configuration for the three-dimensional problem.

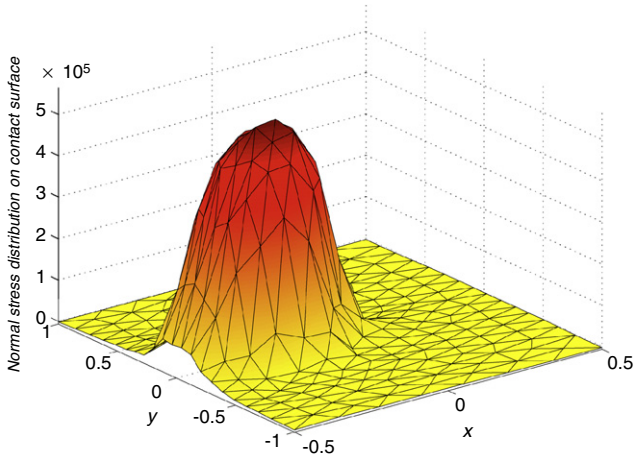

Fig. 10. Normal stress ($\sigma_n(u)$) distribution on Γ_c.

Table 5
Performances of Algorithm UBR-C on the three-dimensional problem.

Mesh nodes Ω/Γ_c	Iterations	CPU (in s)
198/45	36	0.15
739/122	37	0.87
2357/260	40	4.22
10 761/769	40	58.33
17 887/1042	40	129.94

To study the scalability of Algorithm UBR-C, we consider several meshes of different sizes. We report in Table 5 the performances of Algorithm UBR-C. We observe that the number of iterations is virtually independent of mesh size. Note that the timing results in Table 5 do not include the time to assemble the matrix systems; this time is quite significant for three-dimensional systems.

7.2.2. Friction case

An analytical normal pressure is not known for this example. We then use the Lagrange multiplier λ_c^k obtained with Algorithm UBR-C as normal stress and the corresponding approximate friction bound $s_h = \nu_f|\lambda_c^k|$. We report in Table 6 the performances of the Uzawa block relaxation Algorithm UBR-TF and the fixed-point Algorithm CF-FP. We can observe again that the number of iteration is virtually independent of the mesh size. For the largest problem, the computational cost of Algorithm UBR-TF is only (about) 14.5% higher than the frictionless case.

8. Conclusion

We have studied a Uzawa Block Relaxation (UBR) method for a unilateral contact problem with or without friction. The method is developed in the continuous level and easy to implement since both cases (frictionless or the Tresca friction),

Table 6
Performances of Algorithms UBR-TF and CF-FP on the three-dimensional problem.

Mesh nodes Ω/Γ_c	Algorithm UBR-TF		Algorithm CF-FP	
	Iterations	CPU (in s)	Iterations fixed point/Tresca	CPU (in s)
198/45	49	0.23	6/92	0.38
739/122	50	0.90	6/91	1.06
2357/260	45	4.08	6/92	8.83
10 761/769	47	68.42	6/93	122.56
17 887/1042	48	148.66	6/94	266.72

can be incorporated in the same procedure. The main advantage of our method is that the matrix of the linear elasticity subproblem is constant during the iterative process and, therefore, can be factorized only once in the initialization step. Numerical experiments have shown that this property leads to a significant saving of computational cost for large scale problems. In fact, for our largest problem, Algorithm UBR-C is more than 4 times faster than the semi-smooth Newton algorithm SSN-C which exhibits a superlinear rate of convergence but requires a matrix factorization at each iteration.

Even though the Uzawa block relaxation algorithms presented in this paper converge for any $r > 0$, its practical implementation still faces the problem of the optimal choice of the regularization parameter r. Further work is underway for an automatic penalty adjustment procedure.

References

[1] N. Kikuchi, J.T. Oden, Contact Problems in Elasticity: A Study of Variational Inequalities and Finite Element Methods, in: Studies in Applied Mathematics, SIAM, Philadelphia, 1988.
[2] G. Stadler, Infinite-dimensional semi-smooth Newton and augmented Lagrangian methods for friction and contact problems in elasticity, Ph.D. Thesis, Karl-Franzens University of Graz, Graz, Austria, 2004.
[3] P. Wriggers, Computational Contact Mechanics, John Wiley & Sons, 2002.
[4] P.W. Christensen, A. Klarbring, J.S. Pang, N. Strömberg, Formulation and comparison of algorithms for frictional contact problems, Internat. J. Numer. Methods Engrg. (1998) 145–173.
[5] P. Alart, A. Curnier, A mixed formulation for frictional contact problems prone to Newton like solutions methods, Comput. Methods Appl. Mech. Engrg. 92 (1991) 353–375.
[6] P.W. Christensen, J.S. Pang, Frictional contact algorithms based on semi-smooth Newton methods, in: Reformulation: Nonsmooth, Piecewise Smooth, Semi-Smooth and Smoothing Methods, in: Appl. Optim., vol. 22, Kluwer, Dordrecht, 1999, pp. 81–116.
[7] S. Hüeber, G. Stadler, B.I. Wohlmuth, A primal–dual active set algorithm for three-dimensional contact problems with Coulomb friction, SIAM J. Sci. Comput. 30 (2008) 572–596.
[8] H. Khenous, J. Pommier, Y. Renard, Hybrid discretization of the Signorini problem with Coulomb friction, theoretical aspects and comparison of some numerical solvers, Appl. Numer. Math. 56 (2006) 163–192.
[9] A. Klarbring, G. Bjourkman, Solution of large displacement contact problems with friction using Newton's method for generalized equations, Internat. J. Numer. Methods Engrg. 34 (1992) 249–269.
[10] P. Laborde, Y. Renard, Fixed point strategies for elastostatic frictional contact problems, Math. Methods Appl. Sci. 31 (2008) 415–441.
[11] A.Y.T. Leung, G. Chen, W. Chen, Smoothing Newton method for solving two- and three-dimensional frictional contact problems, Internat. J. Numer. Methods Engrg. 41 (1998) 1001–1027.
[12] M. Cocu, Existence of solutions of Signorini problems with friction, Internat. J. Engrg. Sci. 22 (1984) 567–575.
[13] Z. Dostál, J. Haslinger, R. Kučera, Implementation of the fixed point method in contact problems with Coulomb friction based on a dual splitting type technique, J. Comput. Appl. Math. 140 (2002) 245–256.
[14] J. Haslinger, Z. Dostál, R. Kučera, On the splitting type algorithm for the numerical realization of the contact problems with Coulomb friction, Comput. Methods Appl. Mech. Engrg. 191 (2002) 2261–2281.
[15] C. Licht, E. Pratt, M. Raous, Remarks on a numerical method for unilateral contact including friction, in: Unilateral Problems in Structural Analysis, in: Internat. Ser. Numer. Math., vol. 101, Birkhäuser, Nasel, 1991, pp. 129–144.
[16] M. Fortin, R. Glowinski, Augmented Lagrangian Methods: Application to the Numerical Solution of Boundary-Value Problems, North-Holland, Amsterdam, 1983.
[17] R. Glowinski, P. Le Tallec, Augmented Lagrangian and Operator-Splitting Methods in Nonlinear Mechanics, in: Studies in Applied Mathematics, SIAM, Philadelphia, 1989.
[18] D. Kinderlehrer, Remarks about Signorini's problem in linear elasticity, Ann. Sc. Norm. Super. Pisa 4 (1981) 605–645.
[19] D. Bertsekas, Constrained Optimization and Lagrange Multipliers Methods, Academic Press, New York, 1982.
[20] D. Luenberger, Linear and Nonlinear Programming, Addison Wesley, Reading, MA, 1989.
[21] I. Ekland, R. Temam, Convex Analysis and Variational Problems, in: Classics in Applied Mathematics, SIAM, Philadelphia, 1999.
[22] J.T. Hughes, R.M. Ferency, J.O. Halquist, Large-scale vectorized implicit calculations in solid mechanics on a Cray X-MP/48 utilizing EBE preconditioned conjugate gradient, Comput. Methods Appl. Mech. Engrg. 61 (1987) 215–248.
[23] G. Stadler, Path-following and augmented Lagrangian methods for contact problems in linear elasticity, J. Comput. Appl. Math. 203 (2007) 533–547.
[24] K. Ito, K. Kunisch, Semi-smooth Newton methods for variational inequalities of the first kind, M2AN Math. Model. Numer. Anal. 37 (2003) 41–62.
[25] J. Koko, Vectorized Matlab codes for two-dimensional linear elasticity, Sci. Program. 15 (2007) 157–172.
[26] W. Goldsmith, Impact, Edward Arnold, London, 1960.
[27] K. Ito, K. Kunisch, Semi-smooth Newton methods for the Signorini problem, Appl. Math. 53 (2008) 455–568.